Journal of Solid Mechanics Vol. 1, No. 4 (2009) pp. 260-270

Analysis of Wave Motion in a Micropolar Transversely Isotropic Medium

R.R. Gupta*, R. Kumar

Department of Mathematics, Kurukshetra University, Kurukshetra, Haryana 136119, India

Received 25 June 2009; accepted 10 December 2009

ABSTRACT

The present investigation deals with the propagation of waves in a micropolar transversely isotropic layer. Secular equations for symmetric and skew-symmetric modes of wave propagation in completely separate terms are derived. The amplitudes of displacements and microrotation were also obtained. Finally, the numerical solution was carried out for aluminium epoxy material and the dispersion curves. Amplitudes of displacements and microrotation for symmetric and skew-symmetric wave modes are presented to evince the effect of anisotropy. Some particular cases are also deduced.

Keywords: Micropolar; Transversely Isotropic; Amplitude ratios

1 INTRODUCTION

CLASSICAL mechanics deals with the basic assumption that the effect of the microstructure of a material is not essential for describing mechanical behavior. Such an approximation has been shown in many well-known cases. Often, however, discrepancies between the classical theory and experiments are observed, indicating that the microstructure might be important. For example, discrepancies have been found in the stress concentrations in the areas of holes, notches and cracks; elastic vibrations characterized by a high frequency and small wavelengths, particularly in granular composites consisting of stiff inclusions embedded in a weaker matrix, fibers or grains; and the mechanical behavior of complex fluids such as liquid crystals, polymeric suspensions, and animal blood. In general, granular composites, for example porous materials, are widely used in the area of passive noise control as sound absorbers and the effect of acoustical waves characterized by high frequencies and small wavelengths become significant. To explain the fundamental departure of microcontinuum theories from the classical continuum theories, continuum model embedded with microstructures to describe the microscopic motion or a non local model to describe the long range material interaction is developed. This theory extends the application of the continuum model to microscopic space and short-time scales. Micromorphic theory [1, 2] treats a material body as a continuous collection of a large number of deformable particles, with each particle possessing finite size and inner structure. Using assumptions such as infinitesimal deformation and slow motion, Micromorphic theory can be reduced to Mindlin's Microstructure theory [3]. When the microstructure of the material is considered rigid, it becomes the Micropolar theory [4]. Since, Eringen's micropolar takes into account the intrinsic rotation and predict the behavior of material with inner structure, this theory is more appropriate for geological materials like rocks and soils. Different researchers had discussed different type of problems in transversely isotropic elastic material. Abubakar [5] discussed free vibrations of a transversely isotropic plate. Keck et al. [6] derived the frequency equation for the propagation of train of non-torsional axisymmetric harmonic wave in infinitely long shells, made of three concentric cylinders of different transversely isotropic materials. In 1974, Shuvalov et al. [7] described long wavelength onset of the fundamental branches for a free anisotropic plate with arbitrary through plate variation of material properties.

* Corresponding author.
E-mail address: rajani_gupta_83@yahoo.com (R.R. Gupta).

Payton [8] in 1991 has studied wave propagation in a restricted transversely isotropic elastic solid whose slowness surface contains conical points. However, no attempt has been made to study the wave propagation in micropolar transversely isotropic medium.

The aim of the present study is to enhance our knowledge about the propagation of waves in a micropolar transversely isotopic layer. This study has many applications in various fields of science and technology, namely, atomic physics, industrial engineering, thermal power plants, submarine structures, pressure vessel, aerospace, chemical pipes and metallurgy. After developing the solution, frequency equations connecting the phase velocity with wave number, for symmetric and skew-symmetric wave modes are derived. The amplitude ratios of displacements and microrotation are also obtained. The dispersion curves, attenuation coefficients, amplitude ratio of displacements and microrotation for symmetric and skew-symmetric waves are presented and illustrated graphically, to evince the effect of anisotropy.

2 BASIC EQUATIONS

Following Eringen [9], the constitutive relations and balance laws in general micropolar anisotropic medium possessing center of symmetry, in the absence of body forces and body couples, are given by

2.1 Constitutive relations

$$\begin{aligned} t_{ij} &= A_{ijkl}E_{kl} + G_{ijkl}\Psi_{kl} \\ m_{ij} &= G_{ijkl}E_{kl} + B_{ijkl}\Psi_{kl} \end{aligned} \tag{1a}$$

The deformation and wryness tensor are defined by

$$E_{ji} = u_{i,j} + \varepsilon_{ijk}\varphi_k, \quad \Psi_{ij} = \varphi_{i,j} \tag{1b}$$

2.2 Balance laws

$$\begin{aligned} t_{ij,j} &= \rho\ddot{u}_i \\ m_{ik,i} + \varepsilon_{ijk}t_{ij} &= \rho j\ddot{\varphi}_k \end{aligned} \tag{2}$$

where t_{ij} and m_{ij} are respectively, the stress tensor and couple stress tensor, ρ is bulk mass density, u_i and φ_i are respectively the components of displacement vector and microrotation vector. $A_{ijkl,}\, G_{ijkl,}\, B_{ijkl}$ are characteristic constants of material following the symmetry properties given by Eringen [2].

3 PROBLEM FORMULATION AND SOLUTION

We have used appropriate transformations, following Slaughter [9], on the set of Eqs. (1) to derive equations for micropolar transversely isotopic medium and restricted our analysis to the two dimensional problem. In the present paper, we consider an infinite layer with traction free surfaces at $x_3 = \pm 2H$ (layer of thickness 2*H*), which consists of homogeneous, micropolar transversely isotropic material. We take the origin of the coordinate system (x_1, x_2, x_3) on the middle surface of the layer. The $x_1 - x_3$ plane is chosen to coincide with the middle surface and x_3 axis normal to it along the thickness. For the two-dimensional problem, we assume the components of the displacement and microrotation vector of the form

$$\vec{u} = (u_1, 0, u_3), \qquad \vec{\varphi} = (0, \varphi_2, 0) \tag{3}$$

and assume that the solutions are explicitly independent of x_2 i.e. $\partial / \partial x_2 = 0$. Thus the field equations reduce to

$$A_{11}\frac{\partial^2 u_1}{\partial x_1^2}+A_{55}\frac{\partial^2 u_1}{\partial x_3^2}+(A_{13}+A_{56})\frac{\partial^2 u_3}{\partial x_1 \partial x_3}+K_1\frac{\partial \varphi_2}{\partial x_3}=\rho\frac{\partial^2 u_1}{\partial t^2} \tag{4}$$

$$A_{66}\frac{\partial^2 u_3}{\partial x_1^2}+A_{33}\frac{\partial^2 u_3}{\partial x_3^2}+(A_{13}+A_{56})\frac{\partial^2 u_1}{\partial x_1 \partial x_3}+K_2\frac{\partial \varphi_2}{\partial x_1}=\rho\frac{\partial^2 u_3}{\partial t^2} \tag{5}$$

$$B_{77}\frac{\partial^2 \varphi_2}{\partial x_1^2}+B_{66}\frac{\partial^2 \varphi_2}{\partial x_3^2}-K_1\frac{\partial u_1}{\partial x_3}+K_1\frac{\partial \varphi_2}{\partial x_3}=\rho\frac{\partial^2 u_1}{\partial t^2} \tag{6}$$

$$t_{33}=A_{11}\frac{\partial u_1}{\partial x_1}+A_{33}\frac{\partial u_3}{\partial x_3} \tag{7}$$

$$t_{31}=A_{65}\frac{\partial u_3}{\partial x_1}-K_1\varphi_2+A_{55}\frac{\partial u_1}{\partial x_3} \tag{8}$$

$$m_{32}=B_{66}\frac{\partial \varphi_2}{\partial x_3} \tag{9}$$

where $K_1=A_{56}-A_{55}$, $K_2=A_{66}-A_{56}$, and we have used the notations $11\to 1$, $33\to 3$, $12\to 7$, $13\to 6$, and $23\to 5$, for the material constants. For further considerations, it is convenient to introduce the dimensionless variables defined by

$$\begin{aligned}&(x_1',x_3')=\frac{\omega^*}{c_1}(x_1,x_3),\quad (u_1',u_3')=\frac{\omega^*}{c_1}(u_1,u_3),\quad t_{ij}'=\frac{t_{ij}}{A_{55}},\quad m_{ij}'=\frac{m_{ij}c_1}{B_{56}\omega^*},\quad \varphi_2'=\frac{\varphi_2 A_{55}}{K_1},\\ &t'=\omega^* t,\quad \omega^{*2}=\frac{X}{\rho j},\quad c_1^2=\frac{A_{55}}{\rho}\end{aligned} \tag{10}$$

where $X=K_2-K_1$.

4 BOUNDARY CONDITION

The boundaries of the layer are assumed to be stress free. Therefore, we consider the dimensionless boundary conditions at $x_3=\pm H$ as:

$$t_{33}=0,\ \ t_{31}=0,\ \ \ m_{32}=0 \tag{11}$$

5 NORMAL MODE ANALYSIS AND SOLUTION OF THE PROBLEM

We assume the solution for u_1,u_3,φ_2 representing propagating waves in the x_1-x_3 plane of the form

$$(u_1,u_3,\varphi_2)=(1,\bar{u}_3,\bar{\varphi}_2)u_1 e^{i\xi(x_1+mx_3-ct)} \tag{12}$$

where ξ is the wave number, $\omega=\xi c$ is the angular frequency and c is the phase velocity of the wave, m is the unknown parameter which signifies the penetration depth of the wave, $\bar{u}_3,\bar{\varphi}_2$ are respectively, the amplitude ratios of the displacement u_3 and microrotation φ_2 to that of the displacement u_1. With the help of Eqs. (10) and (12), field Eqs. (4)-(6) reduced to (after suppressing primes)

$$\begin{aligned}
&\left[-m^2+(c^2-d_1)-m(d_1+d_2)\overline{u}_3+i\xi m(d_2-1)\overline{\varphi}_2\right]u_1e^{i\xi(x_1+mx_3-ct)}=0\\
&\left[-m\,\xi^2(d_1+d_2)+(m^2-d_3+d_4c^2)\xi^2\overline{u}_3+i\xi(d_2-1)(d_3-d_2d_4)\overline{\varphi}_2\right]u_1e^{i\xi(x_1+mx_3-ct)}=0\\
&\left[i\xi m\,d_7+\frac{i\xi d_7(d_3-d_2d_4)}{d_4(d_2-1)}\overline{u}_3+\left[(m^2-d_5-c^2d_6)\xi^2+d_8\right]\overline{\varphi}_2\right]u_1e^{i\xi(x_1+mx_3-ct)}=0
\end{aligned}\tag{13}$$

where

$$d_1=A_{11}/A_{55},\quad d_2=A_{56}/A_{55},\quad d_3=A_{66}/A_{55},\quad d_4=A_{55}/A_{33},\quad d_5=B_{77}/B_{66},\quad d_6=A_{55}j/B_{66},$$
$$d_7=A_{55}c_1^2/B_{66}\omega^{*2},\quad d_8=K_1/A_{55},\quad d_9=A_{13}/A_{55}$$

The condition for the non trivial solution of system of Eq. (13), yields a cubic equation in m^2 as

$$Am^6+Bm^4+Cm^2+D=0\tag{14}$$

where

$$\begin{aligned}
&A=-\xi^2,\ B=-\xi^2\left[d_3+d_5+d_1-c^2-(d_1+d_2)^2\right]+\omega^2(d_6+d_4)-d_8+d_7(d_2-1)^2,\\
&C=a_2d_7-a_1(c^2d_4-d_3)-(c^2-d_1)(a_1-a_3\xi^2)-a_1(d_1+d_2)^2-a_4\left[(d_1+d_2)(d_3-d_2d_4)a_5+(d_2-1)a_3\right]\\
&D=(c^2-d_1)(c^2d_4-d_3)a_1-d_7a_2(c^2-d_1),\quad a_1=\omega^2d_6-d_5\xi^2-d_8,\quad a_2=(d_3-d_2d_4)^2/d_4,\\
&a_3=d_3-c^2d_4,\quad a_4=d_7(d_2-1),\quad a_5=(d_4+1)/d_4,\quad a_6=a_2,\quad a_7=(d_1-d_2)/(d_2-1)
\end{aligned}$$

The roots of this equation give three values of m^2, and hence of c^2. Three positive values of c will be the velocities of propagation of three possible waves viz quasi-longitudinal displacement (QLD) wave, transverse displacement (QCTD) wave and quasi-coupled quasi-coupled transverse microrotational (QCTM) wave. This fact is verified, when we solve Eq. (14), using MATLAB programming. For isotropic linear micropolar elastic solid i.e., if we put

$$A_{11}=A_{33}=\lambda+2\mu+K,\ A_{55}=A_{66}=\mu+K,\ A_{13}=\lambda,\ A_{56}=\mu,\ K=-K_1=K_2=X/2,\ B_{66}=B_{77}=\gamma$$

In Eq. (14), the velocity c_1 corresponds to longitudinal displacement wave and the velocities c_2 and c_3 correspond to two coupled waves viz transverse microrotational and transverse displacement wave as obtained by Parfitt and Eringen [10]. So Eq. (14) leads to the following solution for displacements and microrotation as:

$$(\overline{u}_1,\overline{u}_3,\overline{\varphi}_2)=\sum_{i=1}^{3}A_i\cos\ (m_ix_3\xi)+B_i\sin\ (m_ix_3\xi)e^{i\xi(x_1-ct)}\tag{15}$$

where

$$r_i=\frac{m_i[(m_i^2\xi^2-a_1)(d_1+d_2)-a_4(d_3-d_2d_4)]}{m_i^4\xi^2-m_i^2(a_1-\xi^2a_3)-a_3a_1-a_6},\qquad t_i=\frac{im_id_7(a_7a_6-m_i^2-a_3)}{m_i^4\xi^2-m_i^2(a_1-\xi^2a_3)-a_3a_1-a_6}\tag{16}$$

6 DERIVATION OF SECULAR EQUATION

Substituting the values of $\overline{u}_1,\overline{u}_3$ and $\overline{\varphi}_2$ in the boundary conditions (11) at the surfaces $\pm H$ of the layer,

$$\begin{aligned}
&\sum_{i=1}^{3}[(g_1c_i - g_{2i}s_i)A_i + (g_1s_i + g_{2i}c_i)B_i] = 0\\
&\sum_{i=1}^{3}[(g_1c_i + g_{2i}s_i)A_i + (-g_1s_i + g_{2i}c_i)B_i] = 0\\
&\sum_{i=1}^{3}[(g_{3i}c_i - g_{4i}s_i)A_i + (g_{3i}s_i + g_{4i}c_i)B_i] = 0\\
&\sum_{i=1}^{3}[(g_{3i}c_i + g_{4i}s_i)A_i + (-g_{3i}s_i + g_{4i}c_i)B_i] = 0\\
&\sum_{i=1}^{3}[-g_{5i}s_iA_i + g_{5i}c_iB_i] = 0\\
&\sum_{i=1}^{3}[g_{5i}s_iA_i + g_{5i}c_iB_i] = 0
\end{aligned} \tag{17}$$

where

$$s_i = \sin\ (m_i\xi x_3)\,,\ c_i = \cos\ (m_i\xi x_3)\,,\ g_1 = d_1 i\xi\,,$$
$$g_{2i} = m_i\xi r_i / d_4,\ \ g_{3i} = i\xi d_2 r_i + (d_2 - 1)^2 t_i,\ \ g_{4i} = \xi m_i\ \ g_{5i} = m_i\xi(d_2 - 1)t_i,\quad i=1, 2, 3$$

In order that the six boundary conditions given by Eq. (11) be satisfied simultaneously, the determinant of the coefficients of A_i and B_i (i=1, 2, 3) in Eqs. (17) vanishes. This gives an equation for the frequency of the layer oscillations. The frequency equation for the waves in the present case, after applying lengthy algebraic reductions and manipulations of the determinant leads to the following secular equations:

$$[T_1]^{\pm} g_1 g_{51}(g_{33} - g_{32}) + [T_2]^{\pm} g_1 g_{52}(g_{31} - g_{33}) + [T_3]^{\pm} g_1 g_{53}(g_{32} - g_{31}) = 0 \tag{18}$$

These are the frequency equations which correspond to the symmetric and skew symmetric mode with respect to the medial plane $x_3 = 0$. Here, the superscript '+' corresponds to skew symmetric and '-' refers to symmetric modes and $T_i = \mathrm{T an}\ (m_i\xi x_3)$, i=1, 2, 3.

6.1 Amplitudes of displacements and microrotation

In this section the amplitudes of displacement components and microrotation for symmetric and skew symmetric modes of plane waves can be obtained as:

$$\begin{aligned}
&[(\overline{u}_1)_{sym}, (\overline{u}_1)_{asym}] = \sum_{i=1}^{3}[A_i\cos(m_i x_3\xi), B_i\sin(m_i x_3\xi)]e^{i\xi(x_1 - ct)}\\
&[(\overline{u}_3)_{sym}, (\overline{u}_3)_{asym}] = \sum_{i=1}^{3} r_i[A_i\sin(m_i x_3\xi), B_i\cos(m_i x_3\xi)]e^{i\xi(x_1 - ct)}\\
&[(\overline{\varphi}_2)_{sym}, (\overline{\varphi}_2)_{asym}] = \sum_{i=1}^{3} t_i[A_i\sin(m_i x_3\xi), B_i\cos(m_i x_3\xi)]e^{i\xi(x_1 - ct)}
\end{aligned} \tag{19}$$

6.2 Specific loss

The specific loss is the ratio of energy (ΔW) dissipated in taking a specimen through a stress cycle, to the elastic energy (W) stored in the specimen when the strain is maximum. Kolsky [11] shows that specific loss $(\Delta W / W)$ is, $_c$times the absolute value of the ratio of the imaginary part of wave number to the real part of wave number i.e.

$$\frac{\Delta W}{W} = 4\pi \left| \frac{\mathrm{Im}(k)}{\mathrm{Re}(k)} \right| \tag{20}$$

He noted that specific loss is the most direct method of defining internal friction for a material.

6.3 Particular case

Taking

$$A_{11} = A_{33} = \lambda + 2\mu + K,\ A_{55} = A_{66} = \mu + K,\ A_{13} = \lambda,\ A_{56} = \mu,\ K = -K_1 = K_2 = X/2,\ B_{66} = B_{77} = \gamma$$

We obtain the corresponding expressions for the micropolar isotropic medium. These results are tally with those obtained in Brulin [12], after changing the dimensionless quantities into physical quantities.

In the limiting case if we neglect the effect of micropolarity, then we will recover the results of classical theory of elasticity for transversely isotropic elastic solid which are similar to those obtained in Abubakar [5] by changing dimensionless quantities into the physical quantities.

By letting $\xi \to \infty$, the secular equations reduced to,

$$c^2 = \frac{b^2 + 1}{m_3^2 + 1},$$

$$a_1^* = d_1 i\xi - \frac{m_i r_i \xi}{d_4}, c_i^* = d_2 i r_i \xi - m_i \xi + (d_2 - 1)^2 s_i, \quad b = -[m_1 s_1 (a_2^* c_3^* - a_3^* c_2^*) + m_2 s_2 (a_3^* c_1^* - a_1^* c_3^*)]$$

7 NUMERICAL RESULTS AND DISCUSSION

In order to illustrate theoretical results obtained in the preceding sections, we now present some numerical results taking

$$A_{11} = 13.8\times10^{10}\,\mathrm{N\,m^{-2}},\ A_{33} = 14.43\times10^{10}\,\mathrm{N\,m^{-2}}, A_{55} = 3.7\times10^{10}\,\mathrm{N\,m^{-2}}, A_{66} = 4.2\times10^{10}\,\mathrm{N\,m^{-2}},$$
$$A_{13} = 8.85\times10^{10}\,\mathrm{N\,m^{-2}}, A_{56} = 2.977\times10^{10}\,\mathrm{N\,m^{-2}}, B_{77} = 3.71\times10^{9}\,\mathrm{N}, B_{66} = 3.9\times10^{9}\,\mathrm{N}$$

For comparison with a micropolar isotropic solid, following Gauthier [13], we take the following values of the relevant parameters for the case of aluminium epoxy composite as,

$$\rho = 2.19\times10^{3}\,\mathrm{Kg\,m^{-3}},\ \lambda = 7.59\times10^{9}\,\mathrm{N\,m^{-2}}, \mu = 1.89\times10^{10}\,\mathrm{N\,m^{-2}}, K = 1.49\times10^{9}\,\mathrm{N\,m^{-2}}$$
$$\gamma = 2.63\times10^{9}\,\mathrm{N},\ j = 0.196\times10^{-2}\,\mathrm{m^2}$$

All numerical computations are carried out by taking $H = 1$. Here, solid line with and without center symbol represent the variations corresponding to micropolar transversely isotropic solid (MTIS) and, for comparison, broken lines with and without center symbol represent the variations corresponding to micropolar isotropic solid (MIS). The lines shown in the figures without center symbol represent the variations corresponding to initial mode $(n = 1)$ of wave propagation, lines with center symbol $(-\mathrm{o}-)$ represent the variations corresponding to second mode

$(n=2)$ and lines with center symbol $(-\Delta-)$ represent the variations corresponding to final mode $(n=3)$ of wave propagation. Figs. 1 and 4 show the variations of phase velocity with respect to R i.e. real part of wave number for symmetric and skew symmetric modes, respectively. It is evident from these figures that for the first mode, the values of phase velocity starts with slight initial increase and then attain a constant value, in both the cases of MTIS and MIS. However, for the higher modes (n=2, 3) its value shows the opposite behavior at initial stage and then represents the similar pattern.

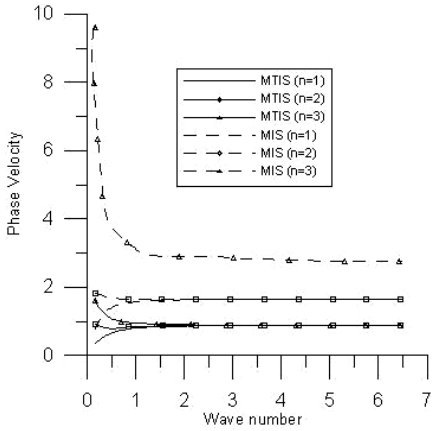

Fig. 1
Variation of phase velocity with wave number for symmetric mode.

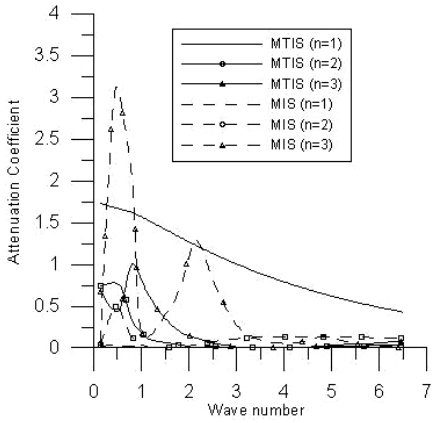

Fig. 2
Variation of attenuation coefficient with wave number for symmetric mode.

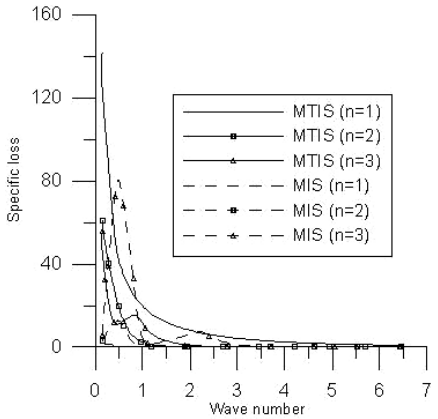

Fig. 3
Variation of specific loss with wave number for symmetric mode.

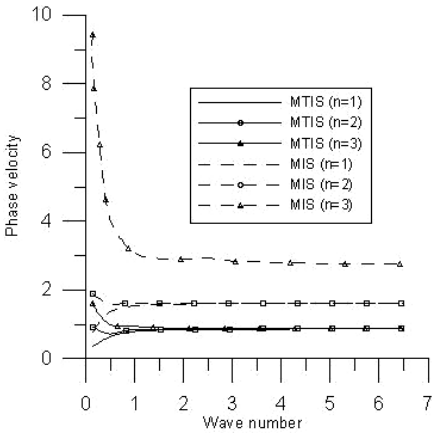

Fig. 4
Variation of phase velocity with wave number for skew symmetric mode.

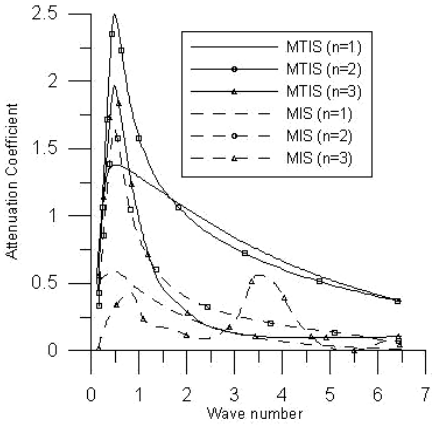

Fig. 5
Variation of attenuation coefficient with wave number for skew symmetric mode.

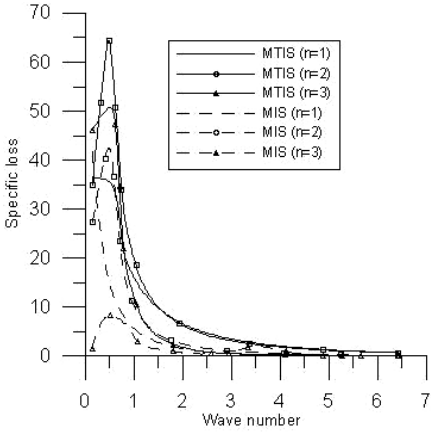

Fig. 6
Variation of specific loss with wave number for skew symmetric mode.

The variation of attenuation coefficient with respect to wave number for symmetric and skew symmetric modes can be depicted from Figs 2 and 5, respectively. It is seen from these figures that for initial mode the value of attenuation coefficient slowly decreases to attain a constant value for MTIS and MIS. As we move to higher mode of wave propagation, its value initially oscillates and then decreases for the case of MTIS. However for MIS and final mode of wave propagation, its value sharply increases and then sharply decreases to attain a peak value within the interval (0, 1) and then becomes constant. For skew symmetric mode, the variation pattern of attenuation coefficient is similar to that of MI for highest mode, with difference in their amplitude and for the lower modes its

value oscillates finitely and becomes constant. The peak value of attenuation coefficient for symmetric mode is higher for third mode of wave propagation but for skew symmetric mode its value is higher for second mode of wave propagation. It can be illustrated from Figs. 3 and 6 that the value of specific loss for initial mode of wave propagation decreases with increase in wave number and tends to attain a constant value, but for the higher modes its value oscillates finitely and becomes constant with increase in wave number. However, for the skew symmetric mode, the trend of variation of specific loss is similar to that of attenuation coefficient. For the range $R > 6$, all the curves approach to vanishingly small values.

Figs. 7-9 indicate the trend of variations of amplitudes of normal displacement, tangential displacement and microrotation with respect to thickness H of the layer. It is depicted from figures 7 and 8 that the amplitude of normal and tangential displacement oscillates finitely within the interval (0, 10) for both symmetric and skew symmetric mode of wave propagation. The amplitudes of oscillation for MTIS are higher as compared to those of MIS. From figure 9, it can be seen that the value of amplitude of microrotation initially decreases and then becomes constant for symmetric mode, while the reverse behavior is observed for skew symmetric mode, as far as the case of MTIS is considered. But for MIS, its value initially increases and then decreases sharply with increase in thickness H of the layer, for the symmetric mode, and for the skew symmetric mode its value initially decreases and then increases over the interval (8, 10). Figs. 10-12 show the variations of phase velocity, attenuation coefficient and specific loss as obtained for the case of Rayleigh wave. In these figures the solid line corresponds to the case of micropolar transversely isotropic half-space, while the dotted line corresponds to the case of micropolar isotropic half-space.

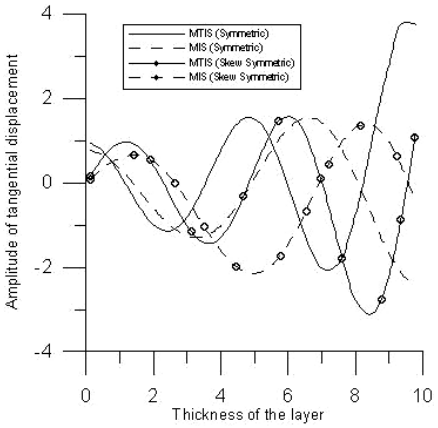

Fig. 7
Variation of amplitude ratio of tangential displacement with thickness H of the layer.

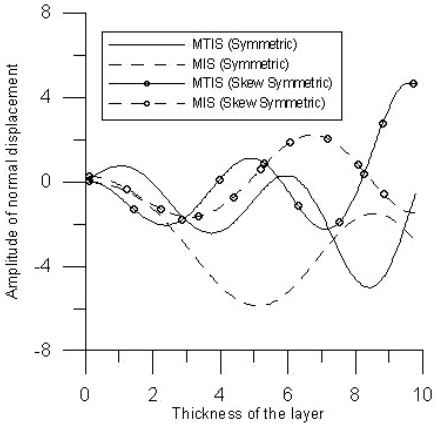

Fig. 8
Variation of amplitude of normal displacement with thickness H of the layer.

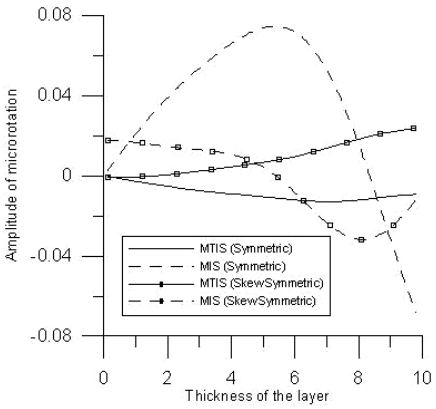

Fig. 9
Variation of amplitude of microrotation with thickness H of the layer.

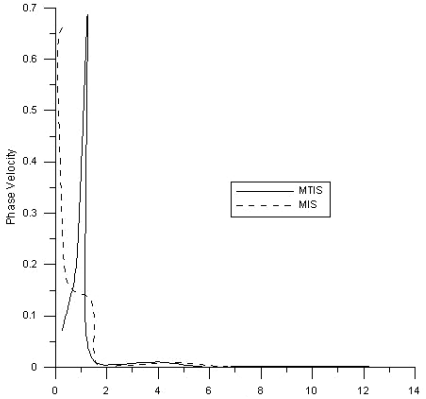

Fig. 10
Variation of phase velocity with wave number.

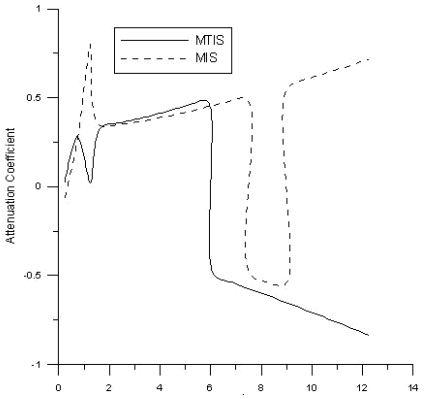

Fig. 11
Variation of attenuation coefficient with wave number.

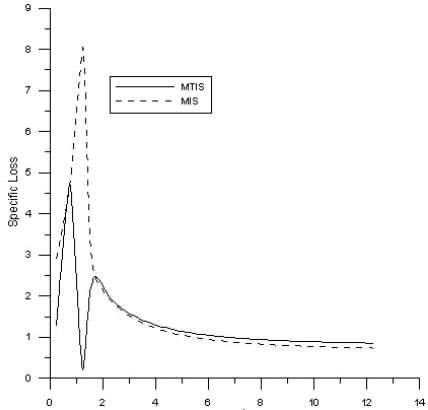

Fig. 12
Variation of specific loss with wave number.

8 CONCLUSIONS

The propagation of waves in an infinite layer of transversely isotropic medium after deriving the secular equation is investigated. The phase velocity of higher modes of wave propagation for symmetric and antisymmetric modes attain quite large values at vanishing wave number, which sharply flattens out to become steady with increasing wave number. The value of attenuation coefficient initially increases and then tends to zero at higher values of wave number. An appreciable of anisotropy is evinced from all the curves. The amplitudes of displacement and specific loss are also computed from the relative expressions and are shown graphically for both symmetric and antisymmetric modes of wave propagation. The numerically computed results are found to be in close agreement with the theoretical results.

RFERENCES

[1] Suhubi E.S., Eringen A.C., 1964, Non-linear theory of simple microelastic solids II, *International Journal of Engineering Science* **2**: 389-404.
[2] Eringen A.C., 1999, *Microcontinuum Field Theories I: Foundations and Solids*, Springer-Verlag, New York.
[3] Mindlin R.D., 1964, Microstructure in linear elasticity, *Archive for Rational Mechanics and Analysis*, **16**: 51-78.
[4] Eringen A.C., 1966, Linear theory of micropolar elasticity, *Journal of Mathematical Mechanics* **15**(6): 909-923.
[5] Abubakar, I., 1962, Free vibrations of a transversely isotropic plate, *Quarterly Journal of Mechanics and Applied* XV, Pt. I: 129-136.
[6] Keck E., Armenkas A.E., 1971, Wave propagation in transversely isotropic layered cylinders, *ASCE Journal of Engineering Mechanics* **2**: 541-555.
[7] Suvalov A.L., Poncelet O., Deschamps M., Baron C., 2005, Long-wavelength dispersion of acoustic waves in transversely inhomogeneous anisotropic plates, *Wave Motion* **42**: 367-382.
[8] Payton R.G., 1992, Wave propagation in a restricted transversely isotropic elastic solid whose slowness surface contains conical points, *Quarterly Journal of Mechanics and Applied* **45**: 183-197.
[9] Slaughter W.S., 2002, *The Linearized Theory of Elasticity*, Birkhauser.
[10] Parfitt Eringen A.C., 1969, Reflection of Plane waves from the flat boundary of a micropolar elastic half-space, *The Journal of Acoustical Society of America* **45**(5): 1258-1272.
[11] Kolsky H., 1963, *Stress Waves in Solids*, Clarendon Press, Oxford; Dover Press, New York.
[12] Brulin O., Hsieh R.K. T., 1981, *Mechanics of Micropolar Media*, World Scientific Publishing Corp. Pvt. Ltd., Singapore.
[13] Gauthier R.D., 1982, Experimental investigations on micropolar media, in: *Mechanics of Micropolar Media*, edited by O. Brulin, RKT Hsieh, World Scientific, Singapore.